

**Whitepaper:
Diffusion Solver in ChiTech**

August, 2018

Jan Vermaak
Rev 1.00



1 Introduction

The “generalized diffusion solver” in Chi-Tech is based on a well known partial differential equation known as the **diffusion equation**. This equation can be used to model the behavior of many physical systems and has been studied in great depth for many years by engineers, scientists and mathematicians. The equation for a single unknown, ϕ , has the general time dependent linear form

$$\frac{d\phi}{dt} = \nabla \cdot (D \nabla \phi) - \sigma \phi + q \quad (1.1)$$

and can be outfitted with a number of different boundary conditions including Dirichlet-type, Neumann-type, and Robin-type boundary conditions. Different spatial discretizations can be applied to the equation including Finite Difference (FD), Finite Volume (FV), Continuous Galerkin (CG), and Discontinuous Galerkin (DG). In Chi-Tech the available spatial discretizations are FV, CG and DG. Additionally, different time discretizations can be applied for which Chi-Tech for now supports Forward Euler, Backward Euler, and Crank-Nicholson.

The steady state form of the diffusion equation will be used in this whitepaper to detail the different spatial discretization techniques and is denoted by

$$-\nabla \cdot (D \nabla \phi) + \sigma \phi = q. \quad (1.2)$$

This equation can be related to techniques contained in literature under certain conditions. When the removal term ($\sigma \phi$) is removed and $D=1$ then the equation becomes Poisson’s equation

$$\nabla \cdot (\nabla \phi) = -q, \quad (1.3)$$

and if the spatial source term, q , is also removed then the equation becomes Laplace’s equation

$$\nabla \cdot (\nabla \phi) = 0. \quad (1.4)$$

In both these forms the divergence of the gradient ($\nabla \cdot \nabla \phi$) is replaced by the Laplacian operator, ∇^2 , which can generally denoted by the symbol Δ after which the following are equivalent

$$\begin{aligned} \nabla \cdot \nabla \phi &= 0 \\ \nabla^2 \phi &= 0 \\ \Delta \phi &= 0 \end{aligned} \quad (1.5)$$

2 Finite Volume

2.1 Discretization

The FV method associates only a single value of the unknown per cell, located at the cell centroid, and is discretized by first integrating equation (1.2) over the cell volume

$$-\int_V \nabla \cdot (D \nabla \phi) dV + \int_V \sigma \phi dV = \int_V q dV \quad (2.1)$$

after which we apply Gauss' divergence theorem to the first term

$$-\int_V \nabla \cdot (D \nabla \phi) dV = -\int_S \mathbf{n} \cdot (D \nabla \phi) dA \quad (2.2)$$

and then apply discretized integration over cell volume, V , and cell face areas, A_f ,

$$-\sum_f \mathbf{A}_f \cdot (D \nabla \phi)_f + V(\sigma \phi) = V q, \quad (2.3)$$

where $\mathbf{A}_f = A_f \mathbf{n}_f$ is the face area vector. This formulation is not complete until we have a discretized expression for $(D \nabla \phi)_f$.

2.1.1 Terminology

Figure 1 below contains a graphic depiction of unstructured 2D cells which we will use to define numerous concepts.

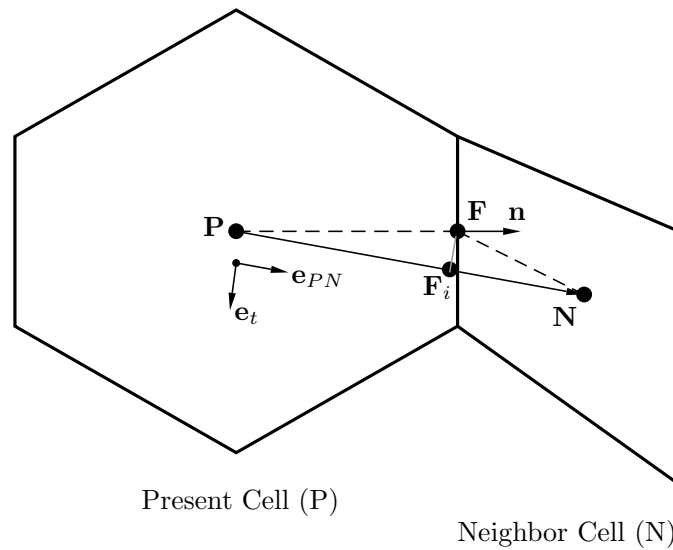


Figure 1: Reference vector layout for neighboring cells

The points \mathbf{P} , \mathbf{N} and \mathbf{F} are the present-cell-, neighboring-cell- and adjoining-face-centroids, respectively. The vector \mathbf{PN} is from \mathbf{P} to \mathbf{N} , and the projection of \mathbf{PF} onto \mathbf{PN} is at point \mathbf{F}_i (not actually at the intersection of \mathbf{PN} with the face). The vector \mathbf{e}_{PN} is the unit vector along \mathbf{PN} computed from \mathbf{PN}/d_{PN} , where $d_{PN} = \|\mathbf{PN}\|_2$. The vector \mathbf{e}_t is the unit tangential vector formed from $\mathbf{e}_t = \mathbf{e}_{PN} - \mathbf{n}$, with \mathbf{n} being the face normal. The distance from \mathbf{P} to \mathbf{F}_i , d_{PF_i} , is computed as $d_{PF_i} = \mathbf{PF} \cdot \mathbf{e}_{PN}$, and $\mathbf{F}_i = \mathbf{P} + d_{PF_i} \mathbf{e}_{PN}$.

2.1.2 Weighted harmonic mean of a quantity D at a face

Some quantities, like the diffusion coefficient, require the harmonic mean at the faces. For unstructured grids this requires a weighted harmonic mean where the weight requires the definition of

$$r_P = \frac{d_{PF_i}}{d_{PN}} \quad (2.4)$$

after which the harmonic mean is defined as

$$D_f = \left(\frac{r_P}{D_P} + \frac{1 - r_P}{D_N} \right)^{-1} \quad (2.5)$$

2.1.3 Flux of a gradient

We can now develop the computation of $\mathbf{A}_f \cdot (D_f \nabla \phi)_f$. When we deal with skewed faces, this diffusion term needs some treatment. In general, since the face is skewed, the flux at the cell face develops additional components other than the orthogonal component along the direction of \mathbf{PN} . These additional components are not intuitive to understand. Refer to Figure 2 below for the following discussion.

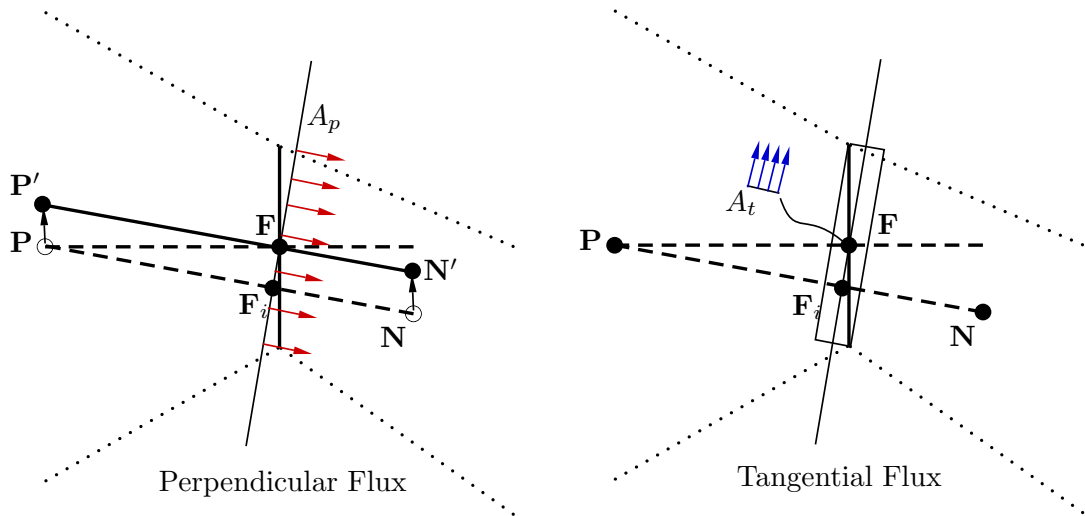


Figure 2: Decomposed areas for the interpolation of a gradient flux

Given that the correct way to approximate the flux across the face is to compute the gradient along its centroid, we require the gradient to be computed from $\phi_{P'}$ and $\phi_{N'}$ along the projected perpendicular area A_p . Additionally we need to compute the flux along the tangential area A_t . Including these terms within an implicit formulation is, however, cumbersome to say the least. Instead we include explicit corrections as described in [2].

Firstly, we formulate the fluxes at \mathbf{P}' and \mathbf{N}' (see the left schematic in Figure 2) as

$$\begin{aligned}\phi_{P'} &= \phi_P + (\nabla\phi)_P^{(n-1)} \cdot \mathbf{F}_i\mathbf{F} \\ \phi_{N'} &= \phi_N + (\nabla\phi)_N^{(n-1)} \cdot \mathbf{F}_i\mathbf{F}\end{aligned}\tag{2.6}$$

where $\mathbf{F}_i\mathbf{F}$ is the vector from \mathbf{F}_i to \mathbf{F} and the gradients are computed from the previous iteration's flux field. The perpendicular gradient term can then be computed from

$$\begin{aligned}\left(\mathbf{A}_f \cdot (\nabla\phi)_f\right)_p &= \frac{A_p}{d_{PN}} \left(\phi_{N'} - \phi_{P'}\right) \\ &= \frac{A_p}{d_{PN}} \left(\phi_N - \phi_P\right) + \frac{A_p}{d_{PN}} \left((\nabla\phi)_N - (\nabla\phi)_P\right)^{(n-1)} \cdot \mathbf{F}_i\mathbf{F}\end{aligned}$$

where $A_p = A_f / (\mathbf{e}_{PN} \cdot \mathbf{n})$. Secondly, the tangential component can be computed from

$$\begin{aligned}\left(\mathbf{A}_f \cdot (\nabla\phi)_f\right)_t &= (\nabla\phi)_F \cdot \mathbf{A}_t \\ &\approx (\nabla\phi)_{F_i}^{(n-1)} \cdot \mathbf{A}_t\end{aligned}\tag{2.7}$$

where $\mathbf{A}_t = \mathbf{A}_f - A_p \mathbf{e}_{PN}$ and the gradient at the face centroid is approximated by the gradient interpolated at \mathbf{F}_i which is not an unreasonable approximation considering that cell skewness is normally minimized. Putting it all together we have

$$\mathbf{A}_f \cdot (\nabla\phi)_f = \frac{A_p}{d_{PN}} \left(\phi_N - \phi_P\right) + \frac{A_p}{d_{PN}} \left((\nabla\phi)_N - (\nabla\phi)_P\right)^{(n-1)} \cdot \mathbf{F}_i\mathbf{F} + (\nabla\phi)_{F_i}^{(n-1)} \cdot \mathbf{A}_t\tag{2.8}$$

In these equations we require the explicit value of $(\nabla\phi)^{n-1}$ which can be computed using different methods, i.e., Green-Gauss and Weighted least-squares. These two methods will now be detailed.

2.1.4 Computing gradients using Green-Gauss

This formulation is identical to “Option 3” of chapter 9.2 in the book by Moukalled et al. [1]. The first order Green-Gauss approximation reduces essentially to a summation over faces.

$$\nabla\phi = \frac{1}{V} \sum_f \mathbf{A}_f \phi_f \quad (2.9)$$

where ϕ_f is taken as a linear interpolation between the adjoining face's cells. This formulation poses some challenges when undetermined faces fluxes are encountered, as is the case with boundaries and unstructured meshes, and therefore we require an algorithm to compensate. Therefore the following algorithm is applied:

1. Compute $\nabla\phi^{(n)}$ over the entire domain using $\frac{1}{V} \sum_f \mathbf{A}_f \phi_f$ where ϕ_f is computed from (??) as

$$\phi_f = (1 - r_P)\phi_P + (r_P)\phi_N + \left[(1 - r_P)\nabla\phi_P + (r_P)\nabla\phi_N \right]^{(n-1)} \cdot \mathbf{F}_i \mathbf{F}$$

and boundary faces are computed as

$$\phi_b = \phi_P + \nabla\phi_P^{(n-1)} \cdot \mathbf{P}\mathbf{F}$$

2. Compute $\|\nabla\phi^{(n)} - \nabla\phi^{(n-1)}\|_2$. If $\|\nabla\phi^{(n)} - \nabla\phi^{(n-1)}\|_2 < \epsilon$ then terminate.
3. Swap $\nabla\phi^{(n)}$ and $\nabla\phi^{(n-1)}$.
4. Repeat 2 to 4.

In most cases the iteration process adds little to the iterative performance and it can be sufficient to just terminate after a single iteration.

2.1.5 Computing gradients using weighted Least-Squares

Section 9.3 in [1] provides a very good description of how the weighted Least-Squares gradients are determined. In that formulation

$$\left\{ \sum_f w_f \mathbf{P}\mathbf{N} \otimes \mathbf{P}\mathbf{N} \right\} \nabla\phi_P = \sum_f \left[w_f \mathbf{P}\mathbf{N} (\phi_N - \phi_P) \right]$$

where

$$w_f = \frac{1}{(\|\mathbf{P}\mathbf{N}\|_2)^2}$$

and the term in $\{\}$ is a tensor. On boundaries, $\mathbf{P}\mathbf{N}$ and ϕ_N is replaced by $\mathbf{P}\mathbf{F}$ and ϕ_b .

Note that this results in a system that needs to be solved for each cell.

2.2 Sparsity pattern

2.2.1 Base block

The parallel sparsity pattern for matrix assembly requires **node ordering** in a single block-sense (base block) as depicted in Figure 3 below. The nodes are cell centered and the base blocks are dependent on the number of cells. The local base block size (i.e., number of entries) is the number of local cells and the global base block size is the total number of cells (globally).

```
auto fv = new SpatialDiscretization_FV;
spatial_discretization = fv;

fv->AddViewOfLocalContinuum(grid);
fv->AddViewOfNeighborContinuums(grid);
fv->ReOrderNodes(grid);
```

After nodal reordering all partition locations will have two populated arrays, `locJ_block_address` and `locJ_block_size`, indexed by partition-id (i.e., processor 15: `locJ_block_address[15]`).

The `locJ_block_address` array contains the global address where each partition's base block starts and the `locJ_block_size` array contains each partitions base block size.

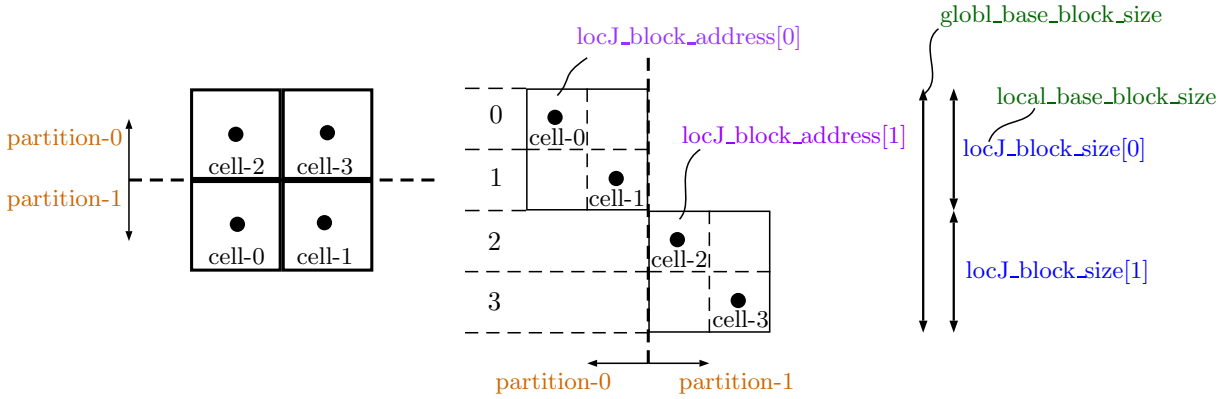


Figure 3: Base block node ordering for the Finite Volume discretization method.

2.2.2 Multiblock

For multiple degrees-of-freedom per node Chi-Tech supports two storage modes: Nodal and Block. Nodal-storage creates a block of unknowns per node, i.e., given a node address, the DOF-addresses will follow sequentially for each unknown. In contrast, Block-storage creates a block for each unknown, i.e., each block contains all the nodes but only a single unknown. The addressing scheme is determined as shown in Figure 4 below which depicts 3 unknown (DOFs) per node. The color coding blue, green and red denotes the particular unknown, i.e., *Velocity-x,y,z*, or *Groups 0,1,2*.

Global IDs	Local IDs	N_{LC} Number of local cells (locJ_block_size)
cell-0	0	N Number of unknowns
cell-1	1	● Unknown $block_{id}$ 0
cell-2	0	● Unknown $block_{id}$ 1
cell-3	1	● Unknown $block_{id}$ 2

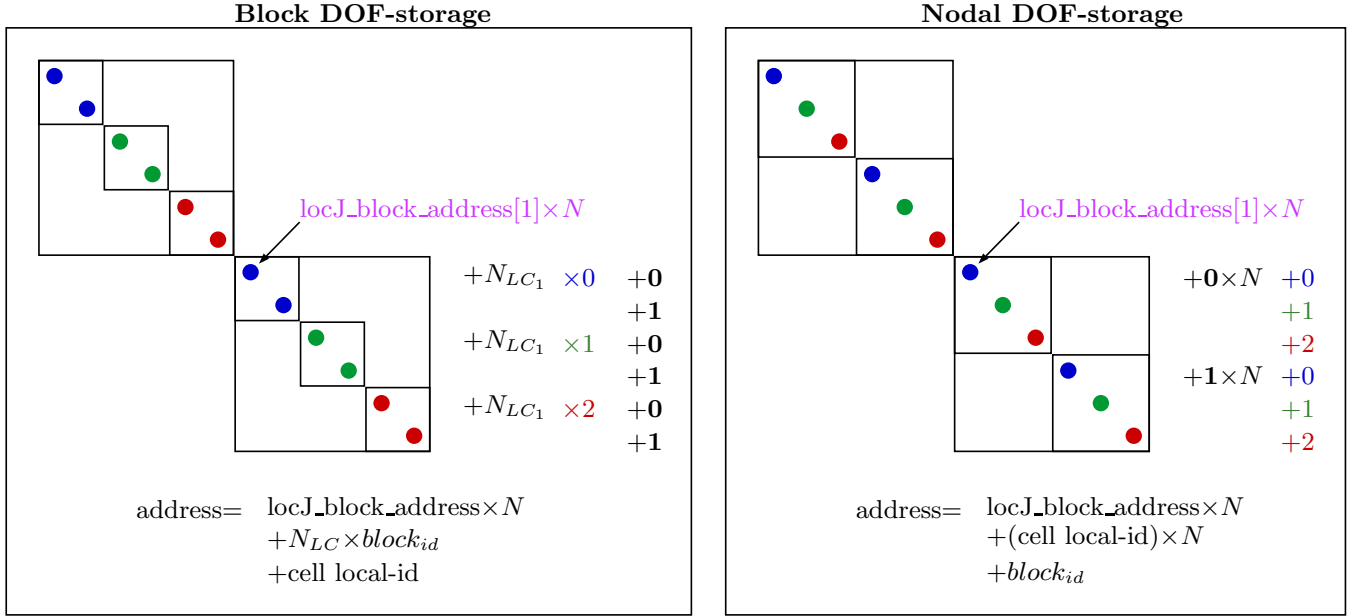


Figure 4: Addressing scheme for multiblock unknowns with the Finite Volume discretization method.

3 The Weak form of the general Diffusion Equation

The diffusion solver handles the solution of the diffusion equation of the form

$$-\nabla(D\nabla\phi) + \sigma_a\phi = q \quad (3.1)$$

over the domain \mathcal{D} and with any set of boundary conditions on the boundary $\partial\mathcal{D}$. This form is suitable for physical processes like heat transfer when $\sigma_a = 0$ and processes like neutron diffusion when $\sigma_a \neq 0$.

We now proceed with multiplying with φ_i , a function mapping eq. 3.1 to a trial space \mathcal{D}_i for which we require that

$$\int_{\mathcal{D}_i} \left(-\varphi_i \nabla(D\nabla\phi) \right) . dV + \int_{\mathcal{D}_i} (\varphi_i \sigma_a \phi) . dV = \int_{\mathcal{D}_i} (\varphi_i q) . dV. \quad (3.2)$$

In this equation we note that, from the product rule we have

$$\begin{aligned} \frac{d(fg)}{dx} &= \frac{df}{dx} \cdot g + f \cdot \frac{dg}{dx} \\ \therefore \int \frac{d(fg)}{dx} . dx &= \int \frac{df}{dx} \cdot g . dx + \int f \cdot \frac{dg}{dx} . dx \end{aligned}$$

Applying this as an analogy with $f = \varphi$ and $g = D\nabla\phi$ we get

$$\begin{aligned} \int_{\mathcal{D}_i} \nabla(\varphi_i D\nabla\phi) . dV &= \int_{\mathcal{D}_i} \nabla\varphi_i \cdot D\nabla\phi . dV + \int_{\mathcal{D}_i} \varphi_i \cdot \nabla(D\nabla\phi) . dV \\ \therefore - \int_{\mathcal{D}_i} \left(\varphi_i \cdot \nabla(D\nabla\phi) . dV \right) &= \int_{\mathcal{D}_i} \nabla\varphi_i \cdot D\nabla\phi . dV - \int_{\mathcal{D}_i} \nabla(\varphi_i D\nabla\phi) . dV \end{aligned} \quad (3.3)$$

Now applying Gauss's Divergence theorem on the last term we have

$$\int_{\mathcal{D}_i} \nabla(\varphi_i D\nabla\phi) . dV = \int_{\partial\mathcal{D}} \hat{n} \cdot \varphi_i D\nabla\phi . dA \quad (3.4)$$

which we can place in equation 3.3 and then subsequently into equation 3.2 which leads to the weak form

$$\boxed{\int_{\mathcal{D}_i} \left(\nabla\varphi_i \cdot D\nabla\phi + \varphi_i \sigma_a \phi \right) . dV - \int_{\partial\mathcal{D}} \left(\hat{n} \cdot \varphi_i D\nabla\phi \right) . dA = \int_{\mathcal{D}_i} (\varphi_i q) . dV.} \quad (3.5)$$

4 Application of basis functions

Consider ϕ approximated by the contributions of basis functions, N_j , and associated coefficients ϕ_j , i.e.

$$\phi \approx \phi_h = \sum_{j=0}^N \phi_j N_j. \quad (4.1)$$

Also consider the source q as being a combination of: a constant-per-element component, q_c , and a non-constant-per-element component, q_{nc} . The non-constant component can then also be expanded using basis functions and coefficients

$$q_{nc} \approx q_{nc,h} = \sum_{j=0}^N q_{nc,j} N_j. \quad (4.2)$$

Equation 3.5 now becomes

$$\begin{aligned} & \int_{\mathcal{D}_i} \left(\nabla \varphi_i \cdot D \nabla \left(\sum_{j=0}^N \phi_j N_j \right) + \varphi_i \sigma_a \left(\sum_{j=0}^N \phi_j N_j \right) \right) dV - \int_{\partial \mathcal{D}} \left(\hat{\mathbf{n}} \cdot \varphi_i D \nabla \left(\sum_{j=0}^N \phi_j N_j \right) \right) dA \\ &= \int_{\mathcal{D}_i} \varphi_i q_c dV + \int_{\mathcal{D}_i} \varphi_i \left(\sum_{j=0}^N q_{nc,j} N_j \right) dV \end{aligned}$$

after which we can move the ∇ operator such that

$$\begin{aligned} & \int_{\mathcal{D}_i} \left(\nabla \varphi_i \cdot D \left(\sum_{j=0}^N \phi_j \nabla N_j \right) + \varphi_i \sigma_a \left(\sum_{j=0}^N \phi_j N_j \right) \right) dV - \int_{\partial \mathcal{D}} \left(\hat{\mathbf{n}} \cdot \varphi_i D \left(\sum_{j=0}^N \phi_j \nabla N_j \right) \right) dA \\ &= \int_{\mathcal{D}_i} \varphi_i q_c dV + \int_{\mathcal{D}_i} \varphi_i \left(\sum_{j=0}^N q_{nc,j} N_j \right) dV \end{aligned}$$

We now take into account that each integral over a trial space \mathcal{D}_i is a summation over all the elements \mathcal{K} that fall within this space. I.e.

Trial space i

$$\begin{aligned} & \sum^K \left[\int_{\mathcal{D}_i} \left(\nabla \varphi_i \cdot D \left(\sum_{j=0}^N \phi_j \nabla N_j \right) + \varphi_i \sigma_a \left(\sum_{j=0}^N \phi_j N_j \right) \right) dV - \int_{\partial \mathcal{D}} \left(\hat{\mathbf{n}} \cdot \varphi_i D \left(\sum_{j=0}^N \phi_j \nabla N_j \right) \right) dA \right] \\ &= \sum^K \left[\int_{\mathcal{D}_i} (\varphi_i q_c) dV + \int_{\mathcal{D}_i} \varphi_i \left(\sum_{j=0}^N q_{nc,j} N_j \right) dV \right] \end{aligned}$$

Rearranging

$$\begin{aligned}
 & \sum_{j=0}^K \sum_{i=0}^N \left[\int_{\mathcal{D}_i} \left(\nabla \varphi_i \cdot D(\phi_j \nabla N_j) + \varphi_i \sigma_a(\phi_j N_j) \right) .dV - \int_{\partial \mathcal{D}} \left(\hat{\mathbf{n}} \cdot \varphi_i D(\phi_j \nabla N_j) \right) .dA \right] \\
 &= \sum_{i=0}^K \left[\int_{\mathcal{D}_i} (\varphi_i q_c) .dV \right] + \sum_{j=0}^K \sum_{i=0}^N \left[\int_{\mathcal{D}_i} \varphi_i (q_{nc,j} N_j) .dV \right] \\
 &\therefore \sum_{j=0}^K \sum_{i=0}^N \phi_j \left[D \int_{\mathcal{D}_i} \nabla \varphi_i \cdot \nabla N_j .dV + \sigma_a \int_{\mathcal{D}_i} \varphi_i N_j .dV - D \hat{\mathbf{n}} \cdot \int_{\partial \mathcal{D}} \varphi_i \nabla N_j .dA \right] \\
 &= \sum_{i=0}^K \left[q_c \int_{\mathcal{D}_i} \varphi_i .dV \right] + \sum_{j=0}^K \sum_{i=0}^N \left[q_{nc,j} \int_{\mathcal{D}_i} \varphi_i N_j .dV \right]
 \end{aligned}$$

By using the same shape functions for the test functions as was used for the basis functions, $\varphi_i = N_i$, we have the following, Galerkin-form of the equations

$$\begin{aligned}
 & \therefore \sum_{j=0}^K \sum_{i=0}^N \phi_j \left[D \int_{\mathcal{D}_i} \nabla N_i \cdot \nabla N_j .dV + \sigma_a \int_{\mathcal{D}_i} N_i N_j .dV - D \hat{\mathbf{n}} \cdot \int_{\partial \mathcal{D}} N_i \nabla N_j .dA \right] \\
 &= \sum_{i=0}^K \left[q_c \int_{\mathcal{D}_i} N_i .dV \right] + \sum_{j=0}^K \sum_{i=0}^N \left[q_{nc,j} \int_{\mathcal{D}_i} N_i N_j .dV \right]
 \end{aligned} \tag{4.3}$$

Computing the integrals of different combinations of the shape functions is specific to the type of element used, i.e. 1D slab, 2D triangle, 2D polygon, 3D tetrahedron, 3D polyhedron, etc. This information is contained in relevant whitepapers.

5 Continuous Finite Element Method (CFEM)

The use of continuous basis functions, as well as the test functions being the same as the basis functions gives rise to the notion of a Galerkin method denoted as the Continuous Finite Element Method (CFEM).

5.1 Assembling the linear system of equations

With each trial space representing an equation, we can assemble a row of a matrix A and an associated entry in the vector \mathbf{b} as

For each element k , for each DOF- i , for each DOF- j

$$a_{ij} = a_{ij} + D \int_{\mathcal{D}_i} \nabla N_i \cdot \nabla N_j \cdot dV + \sigma_a \int_{\mathcal{D}_i} N_i N_j \cdot dV - D \hat{n} \cdot \int_{\partial \mathcal{D}} N_i \nabla N_j \cdot dA \quad (5.1)$$

$$b_i = b_i + q_{nc,j} \int_{\mathcal{D}_i} N_i N_j \cdot dV \quad (5.2)$$

For each element k , for each DOF- i

$$b_i = b_i + q_c \int_{\mathcal{D}_i} N_i \cdot dV \quad (5.3)$$

5.2 Boundary conditions

There are 2 primary types of boundary conditions implemented in ChiTech; **Dirichlet** type boundary conditions and **Robin** type boundary conditions.

5.2.1 Robin and Neumann type boundary conditions

A **Neumann** boundary condition takes the form

$$-D \hat{n} \cdot \nabla \phi = f \quad \text{on } \partial \mathcal{D}$$

where f represents a function. This representation is trivial to implement in the equation for a_{ij} since it essentially means the integral on the boundary is a known and can hence be moved to the right hand side. Hence the equations to do so simply become

$$\begin{aligned} a_{ij} &= a_{ij} + D \int_{\mathcal{D}_i} \nabla N_i \cdot \nabla N_j \cdot dV + \sigma_a \int_{\mathcal{D}_i} N_i N_j \cdot dV - \cancel{D \hat{n} \cdot \int_{\partial \mathcal{D}} N_i \nabla N_j \cdot dA} \\ b_i &= b_i + q_{nc,j} \int_{\mathcal{D}_i} N_i N_j \cdot dV - f_j \int_{\partial \mathcal{D}} N_i N_j \cdot dA \end{aligned}$$

and the rest remaining untouched.

In the case of a **Robin** boundary condition the form is similar;

$$\alpha\phi + \beta D\hat{n} \cdot \nabla\phi = f \quad \text{on } \partial\mathcal{D}$$

however, this time around there is a component still dependent on ϕ which must remain on the left hand side. The equations are

$$\begin{aligned} a_{ij} &= a_{ij} + D \int_{\mathcal{D}_i} \nabla N_i \cdot \nabla N_j .dV + \sigma_a \int_{\mathcal{D}_i} N_i N_j .dV - D \hat{n} \cdot \int_{\partial\mathcal{D}} N_i \nabla N_j .dA + \frac{\alpha}{\beta} \int_{\partial\mathcal{D}} N_i N_j .dA \\ b_i &= b_i + q_{nc,j} \int_{\mathcal{D}_i} N_i N_j .dV + \frac{f_j}{\beta} \int_{\partial\mathcal{D}} N_i b_j .dV \end{aligned}$$

With this notation we can see that by using a Robin boundary condition with $\alpha = 0$ and $\beta = -1$ we can essentially specify a Neumann boundary condition.

The versatility of this boundary condition can also be extended to **Vacuum** boundary conditions in neutron diffusion which take the form

$$\frac{1}{4}\phi + \frac{1}{2}D\hat{n} \cdot \nabla\phi = 0 \quad \text{on } \partial\mathcal{D}$$

representing a zero incoming current. It is simple to see that using the values $\alpha = \frac{1}{4}$, $\beta = \frac{1}{2}$ and $f = 0$ one can specify a vacuum boundary condition using a Robin boundary condition.

5.2.2 Dirichlet type boundary conditions

The Robin type boundary conditions does not have the potential to destroy the symmetry of the matrix. **Dirichlet** boundary conditions on the other hand do have this potential. The Dirichlet boundary conditions takes the simple form

$$\phi = c \quad \text{on } \partial\mathcal{D}.$$

Since none of the weak form equations have components of this form there is only one possible contribution to a_{ij} and that is

$$\begin{aligned} a_{ii} &= 1 & a_{ij} &= 0 \\ b_i &= c \end{aligned}$$

Now, it is fairly trivial in theory to apply this process, however, with the finite element method normally assembling the matrix element-by-element the dirichlet boundary conditions will have to be applied after the element-by-element assembly. Additionally, the dirichlet process zeros out the non-diagonal columns of the given row. This is a problem because the rest of the element-by-element assembly connected other DOFs to the dirichlet DOF via the columns of their respective rows and hence if we do but zero out the non-diagonal components of the matrix row then we are left with a **non-symmetric** matrix.

In ChiTech the whole mess of Dirichlet boundary conditions is handled by modifying the element-by-element assembly process to never connect DOFs to the known dirichlet nodes. For a better understanding of how this is done please consult the coding implementation section.

5.3 Coding implementation

Currently 3 different geometries are implemented in ChiTech. For each geometry a subtle difference needs to be implemented, however, the code sequence is essentially identical. As a reference we will use only a 2D polygon but the overall code implementation is the same for all geometries. Let us now consider a simple 2D arrangement of 4×4 cells as shown in Figure 5 below. The solution is defined on the nodes of the mesh and cells are distributed on processors depicted with colors.

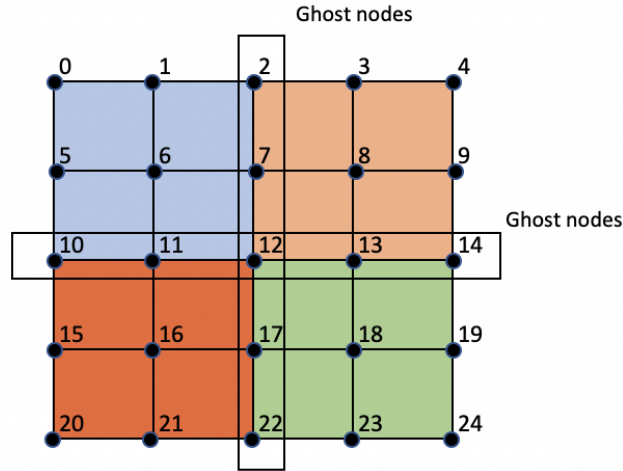


Figure 5: Simple CFEM arrangement of cells colored by processor ownership.

5.3.1 Nodal Reordering

This cell and processor arrangement results in a very disjointed matrix representation which is problematic for most parallel implementations and also results in the matrix having a very large bandwidth. To remedy this a **CFEM nodal re-ordering** is applied to the nodes of the mesh ([ReorderNodesPWL](#)). This process is a two stage process:

Stage 1:

- First all the nodes relevant to a process is collected into a set of exclusive and non-exclusive nodes. This involves a loop over all the degrees of freedom associated with a local cell.

- Another loop is executed over local cells, however, this time we loop over faces and face DOFs. If a face is on a process boundary then node indices associated with all the face DOFs are removed from the exclusive non-exclusive node set and placed in a ghost-node set.
- A ring communication is then used to communicate all the ghost nodes from location i to location $i + 1$ with the last location ending up with the complete list of ghost nodes.
- The last location then broadcasts the completed ghost node set to all other locations.

Stage 2:

- The ghost nodes is broken into $2P - 2$ pieces (2 pieces per location, first and last location gets only 1 piece). If the amount of ghost nodes are not divisible they are stored as the remainder which will get subdivided between the first and last location.
- With this information in hand each processor can determine the portion of the matrix it owns provided it knows the starting row. At this point only the first processor knows its ownership start ... its row 0. Therefore we initiate another ring communication. Each location takes its starting location, adds the local exclusive nodes, then the portion of the ghost nodes its been given and then send the next location its starting location.
- Perform the mapping of original node indexes to distributed node indices.

This process can be visualized as depicted in Figure 6 below. The ordering allows for minimal communication between processes and overall low bandwidth when the amount of rows per processor is small. If further bandwidth reduction is required then a suitable reordering is required per process to reorder the exclusive nodes.

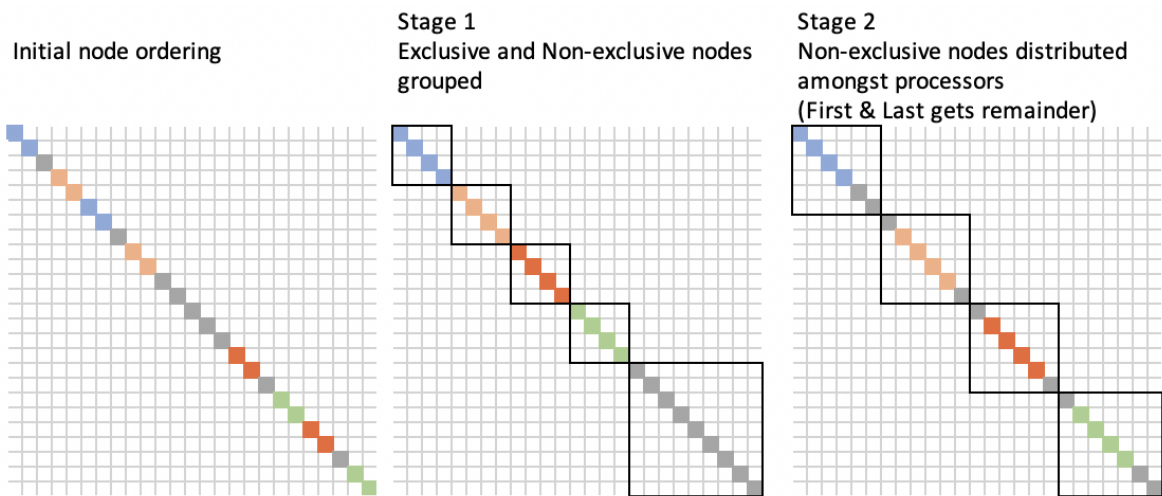


Figure 6: Stages of node ordering for CFEM.

5.3.2 Catching nodes on Dirichlet boundaries

As was discussed in the previous section, the matrix assembly needs to be modified when nodes are on a Dirichlet boundary. Therefore we preprocess the faces to find nodes that are on such boundaries. Note that we loop over faces and only flag nodes if they are on a boundary.

Defined in `diffusion_solver_01c_init_pwlc.cc`

```
//===== Check if i is on boundary
for (int i=0; i<poly_cell->v_indices.size(); i++)
{
    for (int e=0; e<poly_cell->edges.size(); e++)
    {
        if (poly_cell->edges[e][2] < 0)
        {
            int v0_index =
                mesher->MapNode(poly_cell->edges[e][0]);
            int v1_index =
                mesher->MapNode(poly_cell->edges[e][1]);
            if ((ir == v0_index) || (ir == v1_index))
            {
                int boundary_type =
                    boundaries[abs(poly_cell->edges[e][2])-1]->type;
                if (boundary_type == DIFFUSION_DIRICHLET)
                {
                    nodal_boundary_numbers[ir]=poly_cell->edges[e][2];
                }
                break;
            } //if ir part of face
        }
    }
} //for vertices i
```

5.3.3 Estimating the sparsity pattern

In order to improve memory allocation efficiency it is important to have a good estimation of the sparsity pattern of the matrix, specifically the number of non-zeros per row. The estimation is perfect if we can exactly estimate the amount of non-zeros per row, not perfect but good if we over-estimate it and poor if we under-estimate it.

Defined in `diffusion_solver_01c_init_pwlc.cc`

```
//===== Set nodal connections
for (int i=0; i<poly_cell->v_indices.size(); i++)
{
    std::vector<int>* node_links = nodal_connections[ir];
    for (int j=0; j<poly_cell->v_indices.size(); j++)
    {
        int jr = mesher->MapNode(poly_cell->v_indices[j]);

        //===== Check for duplicates
        bool already_there = false;
        for (int k=0; k<node_links->size(); k++)
        {
```



```

        if ((*node_links)[k] == jr)
        {already_there = true; break;}
    }
    if (!already_there)
    {
        (*node_links).push_back(jr);
        if ((jr>=local_rows_from) && (jr<=local_rows_to))
        {
            nodal_nnz_in_diag[ir]+=1;
        }
        else
        {
            nodal_nnz_off_diag[ir]+=1;
        }
    }
} //for j
} //for vertices i

```

After the sparsity pattern has been estimated the matrix preallocation is set using PETSc functions as follows

Defined in `diffusion_solver_01c_init_pwlc.cc`

```

MatMPIAIJSetPreallocation(A,0,&nodal_nnz_in_diag[local_rows_from],
                        0,&nodal_nnz_off_diag[local_rows_from]);
MatSetOption(A, MAT_NEW_NONZERO_ALLOCATION_ERR, PETSC_FALSE);
MatSetOption(A, MAT_IGNORE_ZERO_ENTRIES, PETSC_TRUE);
MatSetUp(A);

```

5.3.4 Assembling the matrix

As part of solver execution the process of assembling the matrix is conducted with reference to the type of geometry dealt with. Again we will be using a 2D polygon for reference. The **volume integrals** and **dirichlet boundaries** are developed using the following code

Defined in `diffusion_solver_02b_0b_polygon.cc`

```

chi_mesh::CellPolygon* poly_cell =
    (chi_mesh::CellPolygon*)(cell);
PolygonFEView* fe_view =
    (PolygonFEView*)pwl_discr->MapFeView(cell_glob_index);

//===== Loop over DOFs
for (int i=0; i<fe_view->dofs; i++)
{
    int ir = mesher->MapNode(poly_cell->v_indices[i]);

    int ir_boundary_type;
    if (!ApplyDirichletI(ir,&ir_boundary_type))
    {
        //===== Develop matrix entry
        for (int j=0; j<fe_view->dofs; j++)
        {
            int jr = mesher->MapNode(poly_cell->v_indices[j]);
            double jr_mat_entry =
                D*fe_view->IntV_gradShapeI_gradShapeJ[i][j];

```

```

    jr_mat_entry +=
        siga*fe_view->IntV_shapeI_shapeJ[i][j];

    int jr_boundary_type;
    if (!ApplyDirichletJ(jr,ir,jr_mat_entry,&jr_boundary_type))
    {
        MatSetValue(A,ir,jr,jr_mat_entry,ADD_VALUES);
    }
} //for j

//===== Develop RHS entry
double rhsvalue =0.0;
rhsvalue = q*fe_view->IntV_shapeI[i];
VecSetValue(b,ir,rhsvalue,ADD_VALUES);
} //if ir not dirichlet
} //for i

```

As can be seen in the above code, if DOF- i is caught to be on a Dirichlet boundary it will be handled by the function [ApplyDirichletI](#).

Defined in [diffusion_solver_01_general.cc](#)

```

bool chi_diffusion::Solver::ApplyDirichletI(int ir,
                                             int *ir_boundary_type,
                                             int iref)
{
    int irefr = iref;
    if (irefr<0)
        irefr = ir;
    //===== Check if i is on boundary
    *ir_boundary_type = NO_BOUNDARY; //NO.BOUNDARY
    int ir_boundary_index= 0;
    if (nodal_boundary_numbers[irefr]<0)
    {
        ir_boundary_index = abs(nodal_boundary_numbers[irefr])-1;
        *ir_boundary_type = boundaries[ir_boundary_index]->type;
    }

    if (*ir_boundary_type == DIFFUSION_DIRICHLET)
    {
        double ir_mat_entry =1.0;
        MatSetValue(A,ir,ir,ir_mat_entry,ADD_VALUES);
        auto dirich_bound =
            (chi_diffusion::BoundaryDirichlet*)boundaries[ir_boundary_index];
        double bvalue = dirich_bound->boundary_value;
        VecSetValue(b,ir,bvalue,ADD_VALUES);
        VecSetValue(x,ir,bvalue,INSERT_VALUES);

        return true; //Applied
    }
    return false; //Not applied
}

```

If a given row i_r has a column connection to a node that is on a Dirichlet boundary then that matrix entry assembly is handled by [ApplyDirichletJ](#).

Defined in `diffusion_solver_01_general.cc`

```
bool chi_diffusion::Solver::ApplyDirichletJ(int jr,int ir,
                                           double jr_mat_entry,
                                           int *jr_boundary_type,int iref)
{
    int irefr = iref;
    if (irefr<0)
        irefr = jr;
    //===== Check if j is on boundary
    *jr_boundary_type = NO_BOUNDARY; //NO.BOUNDARY
    int jr_boundary_index= 1;
    if (nodal_boundary_numbers[irefr]<0)
    {
        jr_boundary_index = abs(nodal_boundary_numbers[irefr])-1;
        *jr_boundary_type = boundaries[jr_boundary_index]->type;
    }

    //===== If not dirichlet then
    if (*jr_boundary_type == DIFFUSION_DIRICHLET)
    {
        auto dirich_bound =
            (chi_diffusion::BoundaryDirichlet*)boundaries[jr_boundary_index];
        double bvalue = -1*jr_mat_entry*dirich_bound->boundary_value;
        VecSetValues(b,1,&ir,&bvalue,ADD_VALUES);

        return true; //Applied
    }//if dirichlet
    return false; //Not applied
}
```

5.3.5 Solving the system

The rest of the process is common to all solvers. PETSc's GAMG is used as a preconditioner and since the matrix is Symmetric Positive Definite (SPD) the Conjugate Gradient solver provides us with superior performance.

Defined in `diffusion_solver_02a_exec.cc`

```
//===== Matrix symmetry check
PetscBool is_symmetric;
ierr = MatIsSymmetric(A,1.0e-4,&is_symmetric);
if (!is_symmetric)
{
    chi_log.Log(LOG_OWARNING)
    << "Assembled matrix is not symmetric";
}

//===== Set up solver
chi_log.Log(LOG_0) << "Diffusion Solver: Solving system\n";
t_solve.Reset();

ierr = KSPCreate(PETSC_COMM_WORLD,&ksp);
ierr = KSPSetOperators(ksp,A,A);

ierr = KSPGetPC(ksp,&pc);
```

```
ierr = PCSetType(pc,PCGAMG);
ierr = PCSetUp(pc);
ierr = KSPSetType(ksp,KSPCG);
ierr = KSPSetTolerances(ksp,1.e-50,residual_tolerance,1.0e50,100);

//===== Set up monitor
ierr = KSPMonitorSet(ksp,&chi_diffusion::KSPMonitorAChiTech,NULL,NULL);

//===== Setup verbose viewer
if (chi_log.GetVerbosity() >= LOG_OVERBOSE_2)
    KSPView(ksp,PETSC_VIEWER_STDOUT_WORLD);

//===== Execute solve
ierr = KSPSetInitialGuessNonzero(ksp,PETSC_TRUE);
ierr = KSPSetUp(ksp);
ierr = KSPSolve(ksp,b,x);CHKERRQ(ierr);
time_solve = t_solve.GetTime()/1000.0;
```

6 CFEM verification

This section establishes a suite of test cases to verify the accurate implementation of the CFEM method. For each dimension we will restrict the domain $r \in [-1, 1]$.

6.1 Slab 1D

Consider the one dimensional problem

$$-\frac{\partial}{\partial x} \frac{\partial \phi}{\partial x} = 1 \quad \forall x \in [-1, 1]$$

We will apply different boundary conditions to test the implementation.

6.1.1 Dirichlet boundary conditions

We now consider the problem

$$\begin{aligned} -\frac{\partial}{\partial x} \frac{\partial \phi}{\partial x} &= 1 \quad \forall x \in [-1, 1] \\ \phi(-1) &= 1 \quad \text{on } \partial\mathcal{D} \\ \phi(1) &= 1 \quad \text{on } \partial\mathcal{D} \end{aligned}$$

which has the analytical solution

$$\phi(x) = -\frac{1}{2}x^2 + \frac{3}{2}$$

A comparison of the solutions is shown in Figure 7. The comparison looks good.

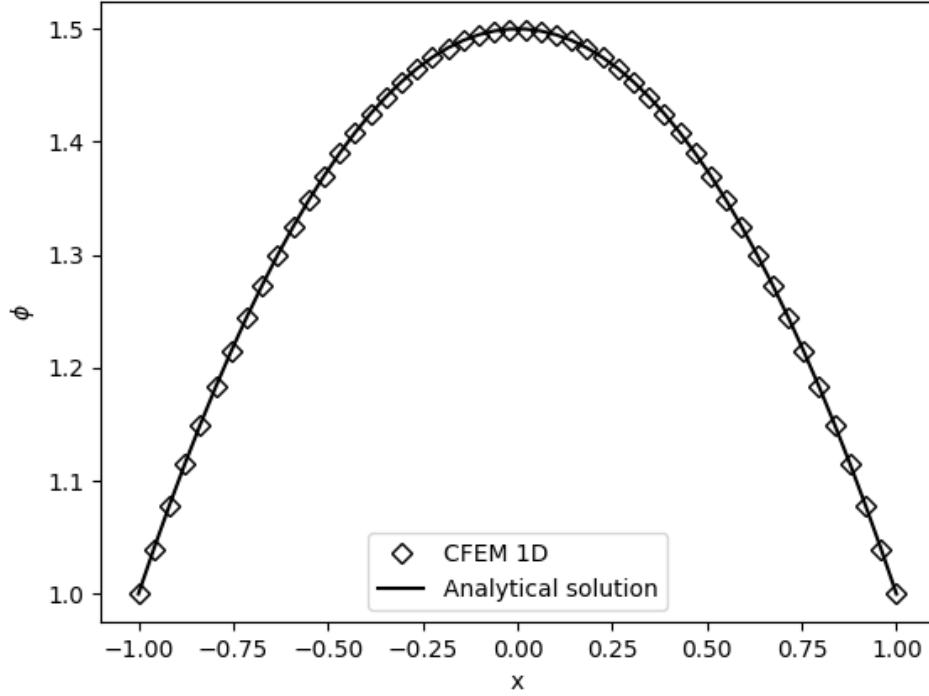


Figure 7: Comparison of CFEM solution to analytical solution.

6.1.2 Reflecting boundary condition

Implementing a reflecting boundary condition cannot involve both boundaries being reflecting or else the system will be indeterminate. Therefore we will take the previous analytical solution and attempt to simulate the right half.

$$\begin{aligned}
 -\frac{\partial}{\partial x} \frac{\partial \phi}{\partial x} &= 1 & \forall x \in [-1, 1] \\
 \frac{\partial \phi}{\partial x} \Big|_{x=0} &= 0 & \text{on } \partial \mathcal{D} \\
 \phi(1) &= 1 & \text{on } \partial \mathcal{D}
 \end{aligned}$$

The analytical solution is still

$$\phi(x) = -\frac{1}{2}x^2 + \frac{3}{2}$$

The results are shown in Figure 8 below.

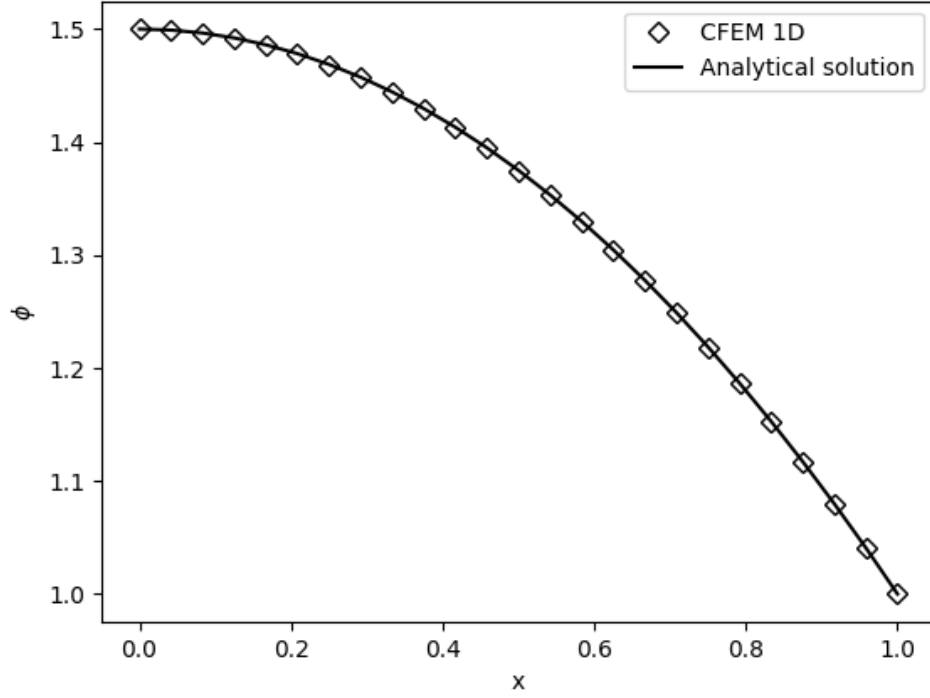


Figure 8: Comparison of CFEM solution to analytical solution using a reflecting boundary.

6.1.3 Vacuum boundary conditions

For vacuum boundary conditions we deal with the following

$$\begin{aligned}
 -\frac{\partial}{\partial x} \frac{\partial \phi}{\partial x} &= 1 \quad \forall x \in [-1, 1] \\
 \frac{1}{4}\phi + \frac{1}{2}D\hat{n} \cdot \frac{\partial \phi}{\partial x} &= 0 \quad \text{on } \partial\mathcal{D}
 \end{aligned}$$

The results are shown in Figure 9.

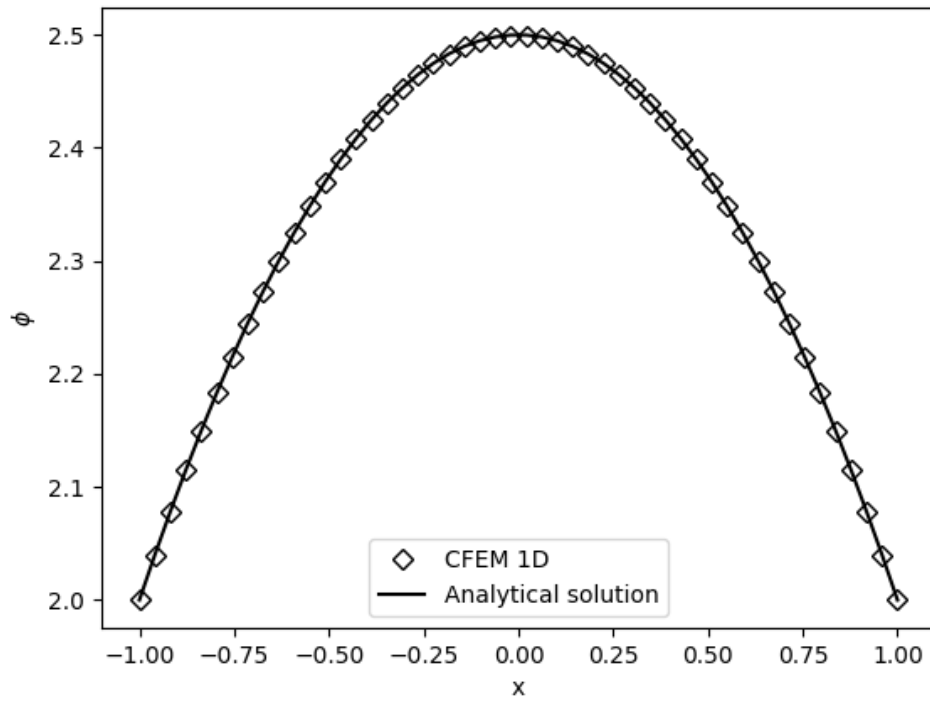


Figure 9: Comparison of CFEM solution to analytical solution using vacuum boundary conditions.

7 Modified Interior Penalty

Instead of a Continuous Finite Element Method (CFEM) discretization, where the solution is defined on nodes, the Discontinuous Finite Element Method (DFEM) stores values per cell. More specifically, using Piecewise Linear (PWL) basis functions and trial functions, defines the solution per cell node. The complication with using this formulation is then that the connectivity between cells is not as easy to determine as it was for CFEM discretization.

The weak form of the diffusion equation is extended as can be observed in the paper by Ragusa, repeated here, the interior penalty method matrix takes on the form

$$\begin{aligned} a(\delta\phi, b_i) &= (\sigma_a \delta\phi, b_i)_{\mathcal{D}} + (D\nabla\delta\phi, \nabla b_i)_{\mathcal{D}} \\ &+ (\kappa^{MIP} \llbracket \delta\phi \rrbracket, \llbracket b_i \rrbracket)_f + (\llbracket \delta\phi \rrbracket, \{\{ D\partial_n b_i \}\})_f + (\{\{ D\partial_n \delta\phi \}\}, \llbracket b_i \rrbracket)_f \\ &+ (\kappa^{MIP} \delta\phi, b_i)_{\partial\mathcal{D}} - \frac{1}{2}(\delta\phi, D\partial_n b_i)_{\partial\mathcal{D}} - \frac{1}{2}(D\partial_n \delta\phi, b_i)_{\partial\mathcal{D}} \end{aligned}$$

where the jump and average operators are defined across an interface as

$$\begin{aligned} \llbracket u \rrbracket &= u^+ - u^- \\ \{\{ u \}\} &= \frac{1}{2}(u^+ + u^-) \end{aligned}$$

The definition of κ^{MIP} is discussed in a later section. The \pm is associated with the sense the given cell has with the given face, i.e. if the face has the righthand-rule convention and consistency with the normal then the cell that has a negative sense to it is the cell to which this convention is consistent. For our purposes we will denote $cell^-$ as the “current”-cell and $cell^+$ as the “adjacent”-cell.

Other notations used here are the volume integrals, $(F)_{\mathcal{D}}$, integration over interior faces $(F)_f$, and integration over face exterior faces $(F)_{\partial\mathcal{D}}$ on the boundary of the domain.

To assemble the matrix entries using this formulation we can replace $\delta\phi$ with b_j to find

$$\begin{aligned} a(b_j, b_i) &= (\sigma_a b_j, b_i)_{\mathcal{D}} + (D\nabla b_j, \nabla b_i)_{\mathcal{D}} \\ &+ (\kappa^{MIP} \llbracket b_j \rrbracket, \llbracket b_i \rrbracket)_f + (\llbracket b_j \rrbracket, \{\{ D\partial_n b_i \}\})_f + (\{\{ D\partial_n b_j \}\}, \llbracket b_i \rrbracket)_f \\ &+ (\kappa^{MIP} b_j, b_i)_{\partial\mathcal{D}} - \frac{1}{2}(b_j, D\partial_n b_i)_{\partial\mathcal{D}} - \frac{1}{2}(D\partial_n b_j, b_i)_{\partial\mathcal{D}} \end{aligned}$$

Let us now develop these terms part-by-part. Imagine 3 terms, corresponding to the terms that have either $\llbracket \cdot \rrbracket$ or $\{\{ \cdot \}\}$, which will be termed part A, B and C.

7.1 Part A

Part A then becomes

$$(\kappa^{MIP} \llbracket b_j \rrbracket, \llbracket b_i \rrbracket)_f = \int_f \kappa^{MIP} \llbracket b_j \rrbracket, \llbracket b_i \rrbracket . dA$$

Now, for simplicity let us replace κ^{MIP} with K and only focus on the terms inside the integral, part A now becomes

$$\begin{aligned} & \kappa^{MIP} \llbracket b_j \rrbracket, \llbracket b_i \rrbracket \\ &= K(b_j^+ - b_j^-)(b_i^+ - b_i^-) \\ &= K(b_i^+ - b_i^-)b_j^+ - K(b_i^+ - b_i^-)b_j^- \\ &= K(b_i^+ - b_i^-)b_j^+ + \boxed{K(b_i^- - b_i^+)b_j^-}. \end{aligned} \tag{7.1}$$

The assembly of the interface terms into the matrix is a very complicated process. Each interface has to update each cell belonging to the interface. This is further complicated by the nominal way in which the matrix is normally assembled, i.e. cell-by-cell. Fortunately, some symmetry exists within the different parts as can be seen in part A above. The boxed portion in the above code is symmetric to the unboxed portion with respect to the cell with a negative sense to the face. In other words if we loop cell by cell and only execute the boxed portion, this will be equivalent to looping over the interfaces and updating both sides.

Given we computed K we can now calculate the following on the interface based on our current cell location ($cell^-$)

$$\begin{aligned} & (\kappa^{MIP} \llbracket b_j \rrbracket, \llbracket b_i \rrbracket)_{E_h^i} \\ & \text{for } i, j \text{ on current cell} \\ & \text{for } i^* \text{ on adjacent cell} \\ & a_{i_r, j_r} = \left[\kappa^{MIP} \int_{S_f} b_i \cdot b_j \cdot dA \right]_{cur-cell} \\ & a_{i_r^*, j_r} = \left[-\kappa^{MIP} \int_{S_f} b_{i^*} \cdot b_j \cdot dA \right]_{adj-cell}, \end{aligned} \tag{7.2}$$

where i_r and j_r refers to the global matrix row and columns as mapped from the local matrices. The coding implementation for this is shown on the next page.

The implementation features a primary loop over trial space i followed by a secondary loop over basis functions j . Since we are dealing only with the shape functions we loop over face dofs and map the face DOFs to cell DOFs using the data **edge_dof_mappings**, developed during FE initialization. We also use the “interior penalty”-view of the cell to determine the matrix row (i_r) corresponding to this cell’s DOF- i . Since we are dealing with b_i^* we also have to determine i_r^* , and hence we determine i_{map} which is the adjacent cell’s DOF- i index that corresponds to the current cell’s DOF- i . The mapping of i_{map} is then

used with the adjacent cell's "interior penalty"-view to map to i_r^* . A similar procedure is applied to the b_j components but this time we are not dealing with indices on the adjacent cell and therefore only j_r is mapped. The values are inserted into global matrix using PETSc's **MatSetValue** which need not refer to local values only.

```
//===== Assemble penalty terms
for (int fi=0; fi<num_face_dofs; fi++)
{
    int i = fe_view->edge_dof_mappings[f][fi];
    int ir = cell_ip_view->MapDof(i);

    //Mapping face index to adj-cell
    int imap = MapCellDof(adj_cell, poly_cell->edges[f][fi]);
    int irstar = adj_ip_view->MapDof(imap);

    for (int fj=0; fj<2; fj++)
    {
        int j = fe_view->edge_dof_mappings[f][fj];
        int jr = cell_ip_view->MapDof(j);

        double aij = kappa*fe_view->IntS_shapeI_shapeJ[f][i][j];

        MatSetValue(A, ir, jr, aij, ADD_VALUES);
        MatSetValue(A, irstar, jr, -aij, ADD_VALUES);
    } //for fj
} //for fi
```

7.2 Part B

Part B is

$$(\llbracket b_j \rrbracket, \{\{D\partial_n b_i\}\})_f = \int_f \llbracket b_j \rrbracket, \{\{D\partial_n b_i\}\} . dA$$

Let us now expand the terms inside the integral

$$\begin{aligned} & \llbracket b_j \rrbracket, \{\{D\partial_n b_i\}\} \\ &= \frac{1}{2} \left(b_j^+ - b_j^- \right) \left(D^+ \hat{n} \cdot \nabla b_i^+ + D^- \hat{n} \cdot \nabla b_i^- \right) \\ &= \frac{1}{2} \left(D^+ \hat{n} \cdot \nabla b_i^+ + D^- \hat{n} \cdot \nabla b_i^- \right) b_j^+ - \frac{1}{2} \left(D^+ \hat{n} \cdot \nabla b_i^+ + D^- \hat{n} \cdot \nabla b_i^- \right) b_j^- \\ &= \frac{1}{2} \left(D^+ \hat{n} \cdot \nabla b_i^+ + D^- \hat{n} \cdot \nabla b_i^- \right) b_j^+ \quad \boxed{-\frac{1}{2} \left(D^+ \hat{n} \cdot \nabla b_i^+ + D^- \hat{n} \cdot \nabla b_i^- \right) b_j^-} \end{aligned}$$

The blocked term in this equation is symmetric to the non-blocked terms with respect to the current cell and the adjacent cell. In other words, the normal (\hat{n}) in the blocked portion is with respect to the current cell ($cell^-$). When we flip the sign of all the \pm denotations and set $\hat{n} = -\hat{n}$ then we obtain the non-blocked

terms. Some of the terms in the blocked portions can be combined with others so let us defer showing the code for that for now and proceed to part C.

7.3 Part C

Part C is

$$(\{\{D\partial_n b_j\}\}, \llbracket b_i \rrbracket)_f = \int_f \{\{D\partial_n b_j\}\}, \llbracket b_i \rrbracket . dA$$

Let us now expand the terms inside the integral

$$\begin{aligned} & \{\{D\partial_n b_j\}\}, \llbracket b_i \rrbracket \\ &= \frac{1}{2} \left(b_i^+ - b_i^- \right) \left(D^+ \hat{n} \cdot \nabla b_j^+ + D^- \hat{n} \cdot \nabla b_j^- \right) \\ &= \frac{1}{2} \left(D^+ \hat{n} \cdot \nabla b_j^+ + D^- \hat{n} \cdot \nabla b_j^- \right) b_i^+ - \frac{1}{2} \left(D^+ \hat{n} \cdot \nabla b_j^+ + D^- \hat{n} \cdot \nabla b_j^- \right) b_i^- \\ &= \frac{1}{2} \left(D^+ \hat{n} \cdot \nabla b_j^+ + D^- \hat{n} \cdot \nabla b_j^- \right) b_i^+ \quad \boxed{-\frac{1}{2} \left(D^+ \hat{n} \cdot \nabla b_j^+ + D^- \hat{n} \cdot \nabla b_j^- \right) b_i^-} \end{aligned}$$

Again the same symmetry applies as with part B (i.e. flipping the denotations and the signs on the normals).

7.4 Assembling B and C

We first look at the blocked parts of B and C together

$$\begin{aligned} & \boxed{-\frac{1}{2} \left(D^+ \hat{n} \cdot \nabla b_i^+ + D^- \hat{n} \cdot \nabla b_i^- \right) b_j^-} \quad \boxed{-\frac{1}{2} \left(D^+ \hat{n} \cdot \nabla b_j^+ + D^- \hat{n} \cdot \nabla b_j^- \right) b_i^-} \\ &= -\frac{1}{2} b_j^- D^+ \hat{n} \cdot \nabla b_i^+ \quad -\frac{1}{2} b_j^- D^- \hat{n} \cdot \nabla b_i^- \quad -\frac{1}{2} b_i^- D^+ \hat{n} \cdot \nabla b_j^+ \quad -\frac{1}{2} b_i^- D^- \hat{n} \cdot \nabla b_j^- \end{aligned}$$

We now reshuffle the terms here after first noting that the second and last terms are the transpose of each other as well as the first and third.

$$= -\frac{1}{2} b_j^- D^- \hat{n} \cdot \nabla b_i^- \quad -\frac{1}{2} b_i^- D^- \hat{n} \cdot \nabla b_j^- \quad -\frac{1}{2} b_j^- D^+ \hat{n} \cdot \nabla b_i^+ \quad -\frac{1}{2} b_i^- D^+ \hat{n} \cdot \nabla b_j^+$$

We now reintroduce the surface integrals

$$\begin{aligned} & \int_f \left[-\frac{1}{2} b_j^- D^- \hat{n} \cdot \nabla b_i^- \quad -\frac{1}{2} b_i^- D^- \hat{n} \cdot \nabla b_j^- \quad -\frac{1}{2} b_j^- D^+ \hat{n} \cdot \nabla b_i^+ \quad -\frac{1}{2} b_i^- D^+ \hat{n} \cdot \nabla b_j^+ \right] . dA \\ &= -\frac{1}{2} D^- \hat{n} \cdot \int_f \left(b_j^- \cdot \nabla b_i^- + b_i^- \cdot \nabla b_j^- \right) . dA \quad -\frac{1}{2} D^+ \hat{n} \cdot \int_f \left(b_j^- \cdot \nabla b_i^+ \right) . dA \quad -\frac{1}{2} D^+ \hat{n} \cdot \int_f \left(b_i^- \cdot \nabla b_j^+ \right) . dA \end{aligned}$$

Theoretically the two right hand integrals could have been lumped in a similar fashion to the left-most integral, however, this segregation proved useful for efficiency in the looping structure with minimal mapping. We therefore have the following three equations to implement

$$a_{i_r,j_r} = -\frac{1}{2}D^- \hat{n} \cdot \int_f \left(b_j^- \cdot \nabla b_i^- + b_i^- \cdot \nabla b_j^- \right) . dA \quad (7.3)$$

$$a_{i_r^*,j_r} = -\frac{1}{2}D^+ \hat{n} \cdot \int_f \left(b_j^- \cdot \nabla b_i^+ \right) . dA \quad (7.4)$$

$$a_{i_r,j_r^*} = -\frac{1}{2}D^+ \hat{n} \cdot \int_f \left(b_i^- \cdot \nabla b_j^+ \right) . dA \quad (7.5)$$

The coding implementation is shown below:

```
// -Di^- bj^- and
// -Dj^- bi^-
for (int i=0; i<fe_view->dofs; i++)
{
    int ir = cell_ip_view->MapDof(i);

    for (int j=0; j<fe_view->dofs; j++)
    {
        int jr = cell_ip_view->MapDof(j);

        double gij =
            n.Dot(fe_view->IntS_shapeI_gradshapeJ[f][i][j] +
                fe_view->IntS_shapeI_gradshapeJ[f][j][i]);
        double aij = -0.5*diffCoeff*gij;

        MatSetValue(A,ir,jr,aij,ADD_VALUES);
    } //for j
} //for i
```

```
// - Di^+ bj^-
for (int imap=0; imap<adj_fe_view->dofs; imap++)
{
    int irmap = adj_ip_view->MapDof(imap);

    for (int fj=0; fj<num_face_dofs; fj++)
    {
        int jmap = MapCellDof(adj_cell,poly_cell->edges[f][fj]);
        int j = MapCellDof(poly_cell,poly_cell->edges[f][fj]);
        int jr = cell_ip_view->MapDof(j);

        double gij =
            n.Dot(adj_fe_view->IntS_shapeI_gradshapeJ[fmap][jmap][imap]);
        double aij = -0.5*diffCoeff*gij;

        MatSetValue(A,irmap,jr,aij,ADD_VALUES);
    } //for j
} //for i
```

```
// - Dj^+ bi^-
for (int jmap=0; jmap<adj_fe_view->dofs; jmap++)
{
    int jrmap = adj_ip_view->MapDof(jmap);

    for (int fi=0; fi<num_face_dofs; fi++)
    {
        int imap = MapCellDof(adj_cell,poly_cell->edges[f][fi]);
        int i    = MapCellDof(poly_cell,poly_cell->edges[f][fi]);
        int ir    = cell_ip_view->MapDof(i);

        double gij =
            n.Dot(adj_fe_view->IntS_shapeI_gradshapeJ[fmap][imap][jmap]);
        double aij = -0.5*diffCoeff*gij;

        MatSetValue(A,ir,jrmap,aij,ADD_VALUES);
    } //for j
} //for i
```

References

- [1] Moukalled F., Mangani L., Darwish M., *The Finite Volume Method in Computational Fluid Dynamics - An Advanced Introduction with OpenFOAM and Matlab*, Springer, 2016.
- [2] Sezai I., *Implementation of boundary conditions in pressure-based finite volume methods on unstructured grids*, Numerical Heat Transfer, Part B: Fundamentals, 2017
- [3] *Blender - a 3D modelling and rendering package*, Blender Online Community, Blender Foundation, Blender Institute, Amsterdam, 2018
- [4] Cheng et al, *Delaunay Mesh Generation*, Chapman & Hall/CRC Computer & Information Science Series, 2013